Preparation of nitric acid modified powder activated carbon to remove trace amount of Ni(II) in aqueous solution

Peidong Su, Junke Zhang, Jiawei Tang and Chunhui Zhang

ABSTRACT

The present study investigated the preparation of nitric acid modified powder activated carbon (MPAC) and its adsorption of trace amounts of Ni(II) from aqueous solution. Results showed that raw powder activated carbon modified with 15% nitric acid (MPAC-15%) had the most developed pore structure and the highest adsorption efficiency for Ni(II) in aqueous solution. For MPAC-15%, the pore width was dominated by micropores with pore width about 1 nm and the total amount of chemical functional groups of MPAC-15% was 0.6630 mmol/g. Ni(II) adsorption tests indicated that the highest adsorption efficiency of MPAC-15% was 98%. The adsorption saturation time of MPAC-15% was about 120 min and the pH-dependent adsorption test showed that neutral conditions ($6.5 < pH < 7.5$) were suitable for Ni(II) adsorption. The adsorption kinetic analysis revealed that the pseudo-second order adsorption model fitted the adsorption process significantly. Thus, Ni(II) adsorption by MPAC-15% was dominated not only by physical adsorption via highly developed micropores but also by chemical adsorption between Ni(II) and surface functional groups. Adsorption isotherm analysis illustrated the Langmuir model was favorable for the adsorption of Ni(II), with $R^2 = 0.9874$.

Key words | activated carbon, adsorption, modification, Ni(II), nitric acid

Peidong Su
Junke Zhang
Department of Civil and Environmental Engineering,
Jackson State University,
Jackson, MS 39217,
USA

Jiawei Tang
Chunhui Zhang (corresponding author)
School of Chemical & Environmental Engineering,
China University of Mining & Technology (Beijing),
Beijing 100083,
China
E-mail: *truemanjung@163.com*

INTRODUCTION

With the increase of industrial activities, a large amount of heavy metal bearing wastes have been released to the water system, which has caused worldwide concern (Porto *et al.* 2017). Nickel, one of the most toxic heavy metals is a non-biodegradable element and, therefore, can present in water persistently. The primary sources of nickel are various industrial processes such as electroplating and battery production (Peng *et al.* 2014). Nickel has been reported to be toxic and carcinogenic if accumulated above the World Health Organization limit of 0.1 mg/L in drinking water. Uptake of excess nickel may lead to development of many diseases (e.g. lung embolism and lung cancer). Therefore, mandated standards and regulations have been issued to minimize nickel contamination in water systems. In China, Beijing has issued a new local standard, DB11/307-2013 Integrated discharge standard of water pollutants', which regulates the discharge limit of nickel (wastewater from workshop or production facility that discharges directly to class II and class III surface water has to meet category A with thresholds of 0.05 mg/L of Ni(II), while discharge to class IV and class V surface water has to meet category B with the limit of 0.4 mg/L of Ni(II)) (MEPBB 2013). Therefore, in order to meet the requirements, environmentally sound and economically viable technologies are required to remove nickel from wastewater.

Activated carbon (AC) adsorption has been proven to be an efficient method, and is widely employed to remove trace metals from wastewater (Kwon *et al.* 2010; Gupta *et al.* 2014). The most important advantages of AC are its high surface area, well-developed internal pore structure and surface chemical functional groups located at the outer and inner surfaces. These characteristics make AC adsorption an attractive approach to remove contaminants in water. However, there are still some reasons to limit its wide application, such as its apolar characteristic that forms during the heating/production process. More importantly,

doi: 10.2166/wst.2019.248

according to the study of Sun *et al.* (2015), the adsorption capacity strongly depends on the pore-filling effect, which means the particle size of the contaminants should be close to the pore size of micropores and/or mesopores. Since the size of metal cations varies from 0.12 (Li^{+}) to 0.338 (Cs^{3+}) nm (Nightingale 1959), it is necessary to modify the AC in proper ways to improve its adsorption of metals. Several surface modification methods can change the AC to more polar materials and change the pore size distribution, such as chemical, physical, microwave treatments and impregnation (Shim *et al.* 2001; Monser & Adhoum 2009; Yao *et al.* 2016; Xiao *et al.* 2017). Among them, chemical surface modification methods are widely used. Former researches indicate that chemical surface modification can enhance the surface functional groups, such as carboxylic, phenolic and lactonic groups, which can improve AC adsorption of trace heavy metals in wastewater treatment (Liu *et al.* 2015; Vunain *et al.* 2016). Li *et al.* (2019) used nitric acid modified AC to remove methyl orange from wastewater and their results indicated that the removal efficiency of methyl orange was about 67%.

Previous studies demonstrated that the amount of oxygen-containing surface functional groups, specific surface area and pore structure are highly related to the concentration of modified agent (Zhang *et al.* 2014; Oladipo & Gazi 2015; Ding *et al.* 2016; Wan & Li 2018). Former researches demonstrated that the higher the reagent concentration, the higher the amount of the surface functional groups of AC would be. Meanwhile, the surface area and pore volume values decrease gradually when the concentrations of the reagent increase (Shim *et al.* 2001; Zhang *et al.* 2015). Thus, there must be a point at which the adsorption capacity of the AC reaches its highest level. Therefore, modification conditions must be well defined to obtain optimal adsorption achievement. Thus, the objective of this article was to prepare optimal modified powder activated carbon (MPAC) with different concentrations of nitric acid and to examine its adsorption of Ni(II) from aqueous solution under various conditions. The adsorption isotherm and kinetic analysis are also determined.

MATERIALS AND METHODS

Materials

Commercial coal-based powder activated carbon (PAC) was purchased from Pingquan Activated Carbon Co., Ltd (Hebei, China). In order to remove the impurities of PAC, 200 g PAC was boiled in purified water for 30 min. After cooling down to room temperature, the PAC was rinsed with purified water several times until the supernatant was transparent. The washed PAC was then dried at 105 ± 5 °C for 24 h.

Concentrated nitric acid (analytical reagent (AR)), nickel sulfate hexahydrate (AR), dimethylglyoxime, methylene blue (HGB3394-60), iodine (AR) and other chemicals were purchased from Sinopharm Chemical Reagent Co., Ltd (Shanghai). All chemicals are standard analytical grade or above. A stock solution with designed concentration of Ni(II) was freshly prepared from nickel sulfate hexahydrate ($NiSO_4{\cdot}6H_2O$) in the laboratory before each use. All solutions in this study were prepared with deionized water.

Preparation of MPAC

Four aliquots of 10 g dried PAC were mixed with 5%, 10%, 15% and 20% (mass fraction) of nitric acid separately at the mass-to-volume ratio of 1:20. After mixing thoroughly, the mixtures were heated to boiling and maintained for 2 h to allow modification to be completed. After cooling down to room temperature, the supernatant was discarded and the residue was rinsed with purified water until no further change in pH. The final products were named as MPAC-5%, MPAC-10%, MPAC-15% and MPAC-20% respectively. All MPACs were dried at 105 ± 5 °C and preserved in a drying cabinet for further tests.

Sample characterization

Iodine value (IV) and methylene blue value (MBV) were measured to investigate the pore size variation according to China standard method GB/T 7702.7-2008 (NEPA 2008a) and China standard method GB/T 7702.6-2008 (NEPA 2008b).

The surface functional groups of PAC and MPACs were determined by Boehm titration method (Ihsanullah *et al.* 2016; Uddin 2017). This method assumes that NaOH neutralizes carboxylic (COOH-), lactonic (RCOOCOR-) and phenolic (PhOH-) groups; Na_2CO_3 neutralizes COOH- and RCOOCOR-; $NaHCO_3$ neutralizes only COOH-; and HCl neutralizes all basic groups. The amount of different types of functional groups was calculated by the amount of titration agent required in the titration.

The Brunauer–Emmett–Teller (BET) surface area, micropore volumes and pore size distribution of the PAC and MPACs were examined by N_2 adsorption/desorption

isotherms at −196 °C through accelerated surface area and porosimetry (ASAP-2020, Micrometrics). All the samples were degassed at 150 °C overnight under 10^{-6} Torr vacuum before testing. The specific surface areas (S_{BET}) were calculated from the N_2 isotherms by applying the BET equation against the relative pressure (P/P_0). The pore size distributions were estimated using the density functional theory method (Moore *et al.* 2001). The surface morphologies of PAC and MPACs were observed with a scanning electron microscope (SEM, JSM-5600LV, JEOL, Japan).

Batch adsorption experiments of Ni(II) solutions

In this study, Ni(II) adsorption tests were performed under various operating conditions. Ni(II) concentration before and after adsorption was determined by China standard method GB 11910-1989 (NEPA 1989). For single adsorption, 1 g PAC or MPACs was mixed with the known concentration of Ni(II) solution at a solid-to-liquid ratio of 1:100 (w/v) in a 250 mL Erlenmeyer flask. A series of Ni(II) concentrations ranging from 0.5 to 8 mg/L were prepared from $NiSO_4{\cdot}6H_2O$ with purified water. The mixture was sealed and shaken on a horizontal vibration shaker at 125 rpm and room temperature for 24 hours. Samples were then taken out and filtered, and the filtrates were stored at 4 °C for further analysis. The Ni(II) concentration was analyzed by a spectrophotometer, Z-7000 (Hitachi, Japan), at a wavelength of 530 nm. The adsorption capacities of Ni(II) for the samples were calculated based on the following equation.

$$q_t \text{ or } q_e = \frac{(C_0 - C_t)V}{M} \tag{1}$$

where q_t or q_e is the adsorption capacity of Ni(II) at time t or equilibrium (mg/g); V is the aqueous volume (L); M is the amount of PAC or MPACs (g); and C_0 and C_t (mg/L) are the initial and equilibrium concentrations of Ni(II) in aqueous solutions respectively. Removal efficiencies of different modified PACs were calculated as:

$$R = \frac{C_0 - C_t}{C_0} \times 100\% \tag{2}$$

Adsorption isotherm and kinetic analysis

To determine adsorption isotherms, 1 g modified AC was utilized with 200 mL Ni(II) solution with initial concentrations ranging from 20 to 200 mg/L at room temperature. Two typical nonlinear adsorption isotherms, Langmuir and Freundlich, were utilized to evaluate the characteristics of the adsorption process. Their corresponding equations are presented as follows (Ghaedi *et al.* 2014; Hu *et al.* 2018).

(1) Langmuir isotherm

$$q_e = \frac{Q_{\max} \cdot K_L \cdot C_e}{1 + K_L \cdot C_e} \tag{3}$$

where $Q_{\max}$ (mg/g) is the maximum amount of Ni(II) that the adsorbent can adsorb, C_e is the equilibrium concentration of Ni(II) (mg/L) and K_L (L/mg) is the Langmuir isotherm constant or energy constant related to the heat of adsorption.

(2) Freundlich isotherm

$$q_e = K_F \cdot C_e^{1/n} \tag{4}$$

where K_F (L/g) is the Freundlich isotherm constant and $1/n$ is the value that is used to indicate the heterogeneity of the adsorbent's surface. As $1/n$ becomes closer to zero, the surface becomes more heterogeneous.

Kinetic analysis discloses the reaction pathways and Ni(II) uptake rate which in turn controls time to reach equilibrium at the solid–liquid interface (Babel & Kurniawan 2004; Yin *et al.* 2007). In order to evaluate adsorption kinetics, time-dependent experiments were conducted using 1 g modified AC with 2 mg/L Ni(II) solution over 120 min. In this study, the adsorption kinetics was fitted by the pseudo-first order model and pseudo-second order model. The equations can be expressed as follows:

$$q_t = q_e\,(1 - e^{-k_1 t}) \tag{5}$$

$$q_t = \frac{k_2 \cdot q_{e^2} \cdot t}{1 + k_2 q_e^t} \tag{6}$$

where q_e (mg/g) and q_t (mg/g) are the amounts of Ni(II) adsorbed at equilibrium and time t, k_1 (min^{-1}) and k_2 (g/(mg·min)) are the rate constants of the pseudo-first order model and pseudo-second order model, respectively.

RESULTS AND DISCUSSION

Characterization of PAC and MPACs

IV and MBV analysis

The IV and MBV results of PAC and MPACs are presented in Table 1. According to the International Union of Pure and Applied Chemistry, there are three classes of pore

Table 1 | Surface functional groups, MBV and IV of PAC and MPACs

Sample	Total acid groups (mmol/g)	$PhOH^-$ (mmol/g)	$COOH^-$ (mmol/g)	Lactone (mmol/g)	MBV (mg/g)	IV (mg/g)
PAC	0.4989	0.173	0.207	0.1189	142.1	559.0
MPAC-5%	0.5162	0.1488	0.2203	0.1471	158.1	695.0
MPAC-10%	0.5774	0.1166	0.2105	0.2503	158.2	660.0
MPAC-15%	0.6630	0.1794	0.2834	0.2002	178.1	688.0
MPAC-20%	0.5900	0.1741	0.2573	0.1586	153.8	658.0

sizes: micropores (diameter (d) < 2 nm), mesopores ($2 \leq d \leq 50$ nm) and macropores (d > 50 nm). It is noted that micropores can be divided into true micropores ($d \leq 0.6$–0.7 nm) and sub-micropores (0.6–$0.7 \text{ nm} \leq d \leq 1.5$–$1.6$ nm). Several researches indicated the iodine molecule has a molecule diameter about 0.532 nm and methylene blue has a diameter about 1.1–1.2 nm; therefore, IV and MBV estimate the value of micropores and sub-micropores in PAC and MPACs, and are two important indicators of adsorbent porosity characteristics in water treatment.

From Table 1, MPACs provided higher MBV and IV than raw PAC. MBV of the MPAC samples varied from 153.8 to 178.1 mg/g after modification, while PAC had 124.1 mg/g MBV. At the same time, IVs in MPACs were about 658–695 mg/g against 559 mg/g for PAC. As aforementioned, IV reflects the microporous structure and MBV reflects the sub-micropores of AC. Indeed, the ratio of micropores to total pores increased by 2–9%, obtained form the values in Table 2. Therefore, it is reasonable that nitric acid modification made a contribution to the development of micropores.

Surface functional groups

The amount of surface functional groups from Boehm titration tests of the PAC and MPACs is summarized in Table 1. The values were calculated by the Boehm titration tests results divided by the mass of the solid samples.

It can be seen in Table 1 that the total acid groups of MPACs was higher than that of original PAC; this is in agreement with the study by Babel & Kurniawan (2004). Among the MPACs, MPAC-15% had total acid groups of 0.6630 mmol/g which was much higher than that of PAC (0.4989 mmol/g). The same trend happened for COOH- of MPACs and the maximum amount of COOH- was 0.2834 mmol/g for MPAC-15%. For PhOH-, it is noted that only the PhOH- amounts of MPAC-15% and MPAC-20% were in the proximity of the amount in original PAC with 0.173 mmol/g, while the other two were both lower than that of PAC. According to Gokce & Aktas (2014), the amount of surface functional groups of nitric acid modified AC followed the order of: COOH- > lactone > PhOH-. Combined with the variations of COOH- and PhOH-, it can be concluded that when nitric acid concentration ranged from 5% to 10%, the original PhOH- of the PAC reacted with COOH- formed by modification to generate lactone groups and therefore there was a significant decrease of PhOH- amount and increase of lactone amount. Along with the nitric acid concentration increasing, the increase rate of COOH- was higher than that of PhOH-. Therefore, the PhOH- amount of MPAC-15% and MPAC-20% was close to the amount of PAC. The lactone amount in all MPACs was higher than that in the PAC.

Surface characteristics

In order to verify surface property changes of the samples, BET-N_2 gas adsorption/desorption isotherm was obtained to reveal the surface area and pore property variation and the results are given in Table 2 and Figure 1.

Table 2 | Pore characteristics of PAC and MPACs

Sample	Surface area (m^2/g)	Total pore volume (cm^3/g)	Average pore size (nm)	Mesopore volume (cm^3/g)	Micropore volume (cm^3/g)	$V_{micropore}/V_{total}$ (%)
PAC	682.1	0.372	2.297	0.124	0.248	63.23
MPAC-5%	754.9	0.449	2.251	0.135	0.314	69.90
MPAC-10%	759.0	0.461	2.432	0.157	0.304	65.97
MPAC-15%	770.0	0.429	2.274	0.132	0.297	69.25
MPAC-20%	765.3	0.433	2.262	0.125	0.308	71.11

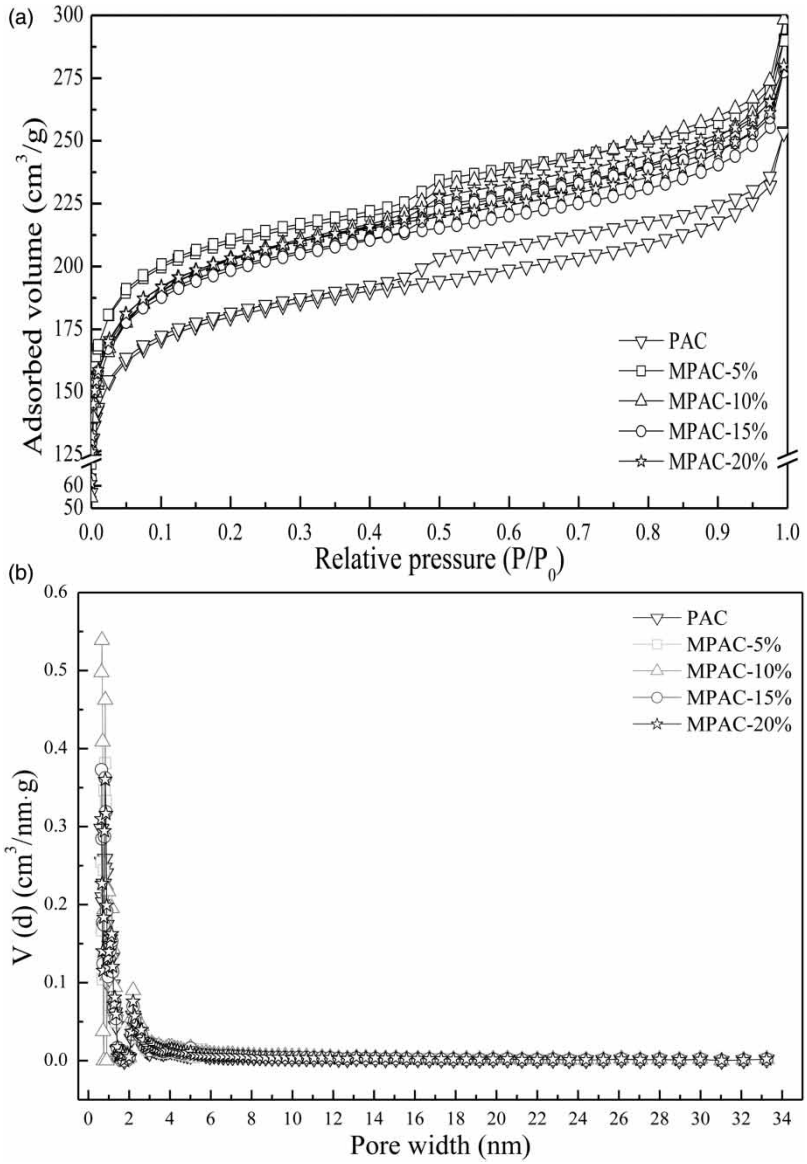

Figure 1 | (a) Isotherms of N_2 adsorption and desorption, and (b) pore width distribution.

From Table 2, the surface areas followed the order of $S_{MPAC\text{-}15\%} > S_{MPAC\text{-}20\%} > S_{MPAC\text{-}10\%} > S_{MPAC\text{-}5\%} > S_{PAC}$, indicating that pore structure of MPACs was well developed compared to PAC. This could be caused by the nitric acid modification enhancing the porosity of the raw PAC. The maximum surface area of 770.0 m^2/g of MPAC-15% was much higher than that of PAC with 682.1 m^2/g. It was also clear that increased total pore volume after modification provides MPACs more adsorption sites for contaminants. The mesopore volume increased slightly along with the nitric acid concentration increasing except for MPAC-20%. The significantly increased micropore volume after modification proved that nitric acid modification can facilitate the texture properties of AC. Moreover, the relatively high proportions of micropores mean that nitric acid had a considerable effect on micropore development. As shown in Table 2, micropore volume occupied 71.11% of the total pore volume for MPAC-20%, while this number for PAC was 63.23%. Thus, MPACs provided more sites for adsorption of small particles (i.e. Ni^{2+} ions or iodine).

To evaluate the effect of different nitric acid concentrations on the modification of PAC, the N_2 adsorption/desorption isotherms and pore size distributions have been investigated. As Figure 1(a) shows, generally, the adsorbed volume of nitrogen gas increased with the relative pressure increasing. When the relative pressure varied from 0 to

0.05, the N_2 adsorption/desorption curves dramatically changed for all the adsorbents. This indicated the isotherm in this P/P_0 range was governed by a Type I isotherm and micropores made a great contribution to the adsorption of N_2. As presented in Table 2, the average pore size for all the adsorbents was around 2.3 nm, which is near the range of micropores, making the results in Figure 1(a) more explainable. Moreover, according to former studies, the uptakes are dominated by the accessible micropore volume rather than by the internal surface area (Sing 1985). When the relative pressure was between 0.05 and 0.45, the curves slowly went up suggesting that there was no significant change in nitrogen gas adsorption/desorption during this range. When the relative pressure was higher than 0.45, there was a hysteresis loop until the relative pressure became close to 1.0, revealing the existence of mesopores (Yang *et al.* 2016). This phenomenon indicated that the isotherm of PAC and MPACs belong to Type IV and its hysteresis loop is strongly associated with capillary condensation taking place in mesopores. The main reason for this phenomenon could be that mesoporous capillary condensation is obvious among this pressure range (Rivera-Utrilla *et al.* 2011). Compared to all the curves obtained from the tests, it can be found that the adsorption volumes of MPACs were larger than PAC, and MPAC-15% achieved the highest pore volumes. From Table 2, MPAC-15% had the highest surface area at the same time. With the increase of acid concentration for modification, the pore volume from the N_2 adsorption/desorption isotherm and surface area slightly decreased in MPAC-20%. This indicated the nitric acid as modification agent can develop the pores very well at optimal concentration, while extremely high concentration would destroy the newly formed pores, thus decreasing pore volume.

The pore size distribution of the samples is given in Figure 1(b). It can be observed that all the samples had similar pore size distribution and both PAC and MPACs were dominated by micropores with a pore size of 1 nm. After modified by nitric acid, the mesopores and micropores in MPACs were both increased, as the peaks of MPACs being higher than that of PAC. However, peaks appeared at about 2–2.5 nm indicating that the increases of micropore and mesopore amount were not necessarily proportional to the total pore amount in each sample (Shafeeyan *et al.* 2010; Kong *et al.* 2018).

Morphological characterization of PAC and MPAC-15%

Based on the analysis of pore characteristics of the samples as mentioned above, MPAC-15% was chosen as the adsorbent to remove Ni(II) ions from aqueous solutions. SEM analysis was performed on both raw PAC and MPAC-15% and the results are presented in Figure 2. Obviously, there are significant differences between these two samples. The raw PAC showed a featureless surface and there was no obvious and regular pore on the surface, while the morphology of MPAC-15% was obviously destroyed and became uneven with a lot of newly created cavities. These

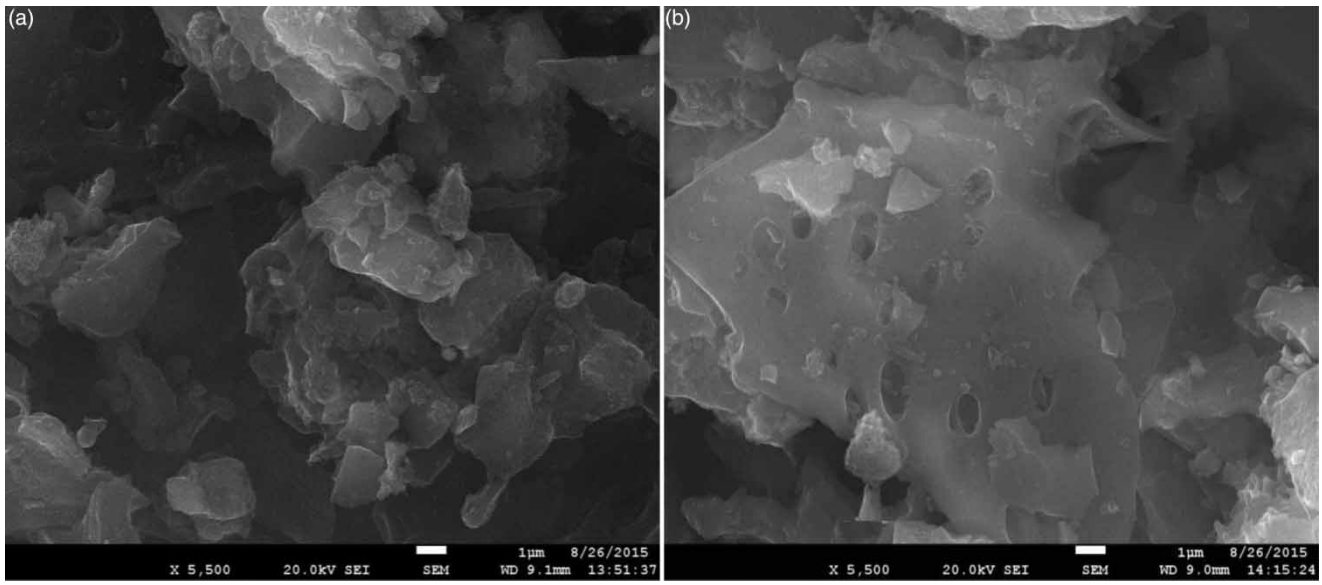

Figure 2 | SEM images of (a) PAC and (b) MPAC-15%.

differences could result from nitric acid which oxidized original carbon on the surface of PAC. These changes greatly contributed to the development of pores, thus increasing the contact area and facilitating mass transfer during adsorption. The surface of MPACs also indicated nitric acid posed significant positive effects on the modification of PAC.

Ni adsorption analysis

Effect of MPAC types

In the Ni(II) adsorption test, an aliquot of 1 g adsorbent was added into 200 mL Ni(II) solutions with the concentrations varying from 0.5 to 8 mg/L and the results are presented in Figure 3(a). As the Ni(II) concentrations ranged from 0.5 to 2 mg/L, the adsorption efficiency increased overall. This could be because there were not enough adsorption sites on the adsorbent, and the concentrations of Ni(II) were so low that the adsorption limit was not reached. With the Ni(II) concentration increasing from 2 to 4 mg/L, the Ni removal efficiency of MPAC-10%, MPAC-15% and MPAC-20% had no significant change, as the Ni(II) adsorption efficiencies were all higher than 90%. When the Ni(II) concentrations ranged from 4 to 8 mg/L, the adsorption efficiency of all the samples become steady with slight fluctuation. Considering the average adsorption performance under all ranges of Ni(II) concentrations, MPAC-15% behaves better as the results were relatively stable and slightly higher. To summarize the results, MPACs achieved higher adsorption efficiencies than original PAC, and the capacities increased in general as the percentage of nitric acid increased during the modification. This could be caused by the more negatively charged surface of MPACs than PAC due to the acid functional groups. The acid groups can behave as ion exchangers, retaining the Ni(II) while releasing the H^+ into solution. Moreover, the dissociation of these groups can enhance electrostatic interaction between MPACs and Ni(II) (Bhatnagar *et al.* 2013). Normally, 2 mol H^+ can be replaced by 1 mol of Ni(II); in this case, the more the total acid functional groups the higher the Ni(II) adsorption efficiency.

Effect of contact time

In order to determine the adsorption saturation time, 1 g MPAC-15% was added to 2 mg/L Ni(II) solution with a total volume of 200 mL. The result is presented in Figure 3(b). From 10 to 60 min, the concentration of Ni(II) decreased sharply revealing that MPAC-15% can significantly adsorb Ni(II) from the solution during this period. This was reasonable because of the abundant pore sites and chemical functional groups existing on the MPAC-15% surface. From 60 to 120 min, the concentration of Ni(II) decreased from 0.26 mg/L to 0.13 mg/L. This could be caused by the fewer number of available pores available for Ni(II) adsorption. After 120 min of adsorption, the concentration of Ni(II) became steady with a concentration of 0.13 mg/L, meaning MPAC-15% achieved its adsorption saturation point. Therefore, the saturation time of MPAC-15% adsorption of Ni(II) was about 120 min, at which the maximum adsorption efficiency was 93.5%.

Effect of pH

pH is an important factor that affects treatment efficiency of Ni(II) in aqueous solution. The solubility of Ni(II) compounds varies at different pH range, i.e. the solubility of $Ni(OH)_2$ becomes very low when pH > 9 and the concentration of Ni(II) will actually be governed by Ni^{2+} ions in the course of acidic conditions (Hummel & Curti 2003; Su *et al.* 2019). When pH varied from 2 to 14, Ni(II) existed in five different forms (Ni^{2+}, $Ni(OH)^+$, $Ni(OH)_2$, $Ni(OH)_3^-$ and $Ni(OH)_4^{2-}$) in liquid as presented in Figure 3(d). Thus, in this study, a pH gradient from 3.2 to 11.2 was selected to investigate the effect of pH on Ni(II) removal by MPAC-15%. As Figure 3(c) shows, when pH was 3.2, the final concentration of Ni(II) was close to the initial value. As discussed above, MPAC-15% surface was functional sited by carboxylic (COOH-) groups and hydroxyl (PhOH-) groups. Under acidic condition, the surface of MPAC-15% was positive and highly protonated with hydrogen ions (H^+). The H^+ on the surface would exchange and compete with Ni(II) on the adsorption sites. In the case of exchange and competition process coexisting, the electrostatic repulsion between cations-Ni(II) and H^+ was conspicuous. Thus, lower pH led to lower adsorption capacities and removal efficiencies as Figure 3(c) shows. As pH increased, the Ni(II) concentration decreased, and thus the adsorption efficiency went high. When pH was 6.7, the equilibrium adsorption capacity was 0.38 mg/g and the removal efficiency reached 95%. This is acceptable because at this pH over 90% Ni(II) was formed as Ni^{2+} ions which were more prone to be adsorbed. In addition, under neutral conditions, the electrostatic repulsion of H^+ weakened, and competition between Ni^{2+} and H^+ diminished. The overall adsorption capacities and removal efficiencies under base condition were much

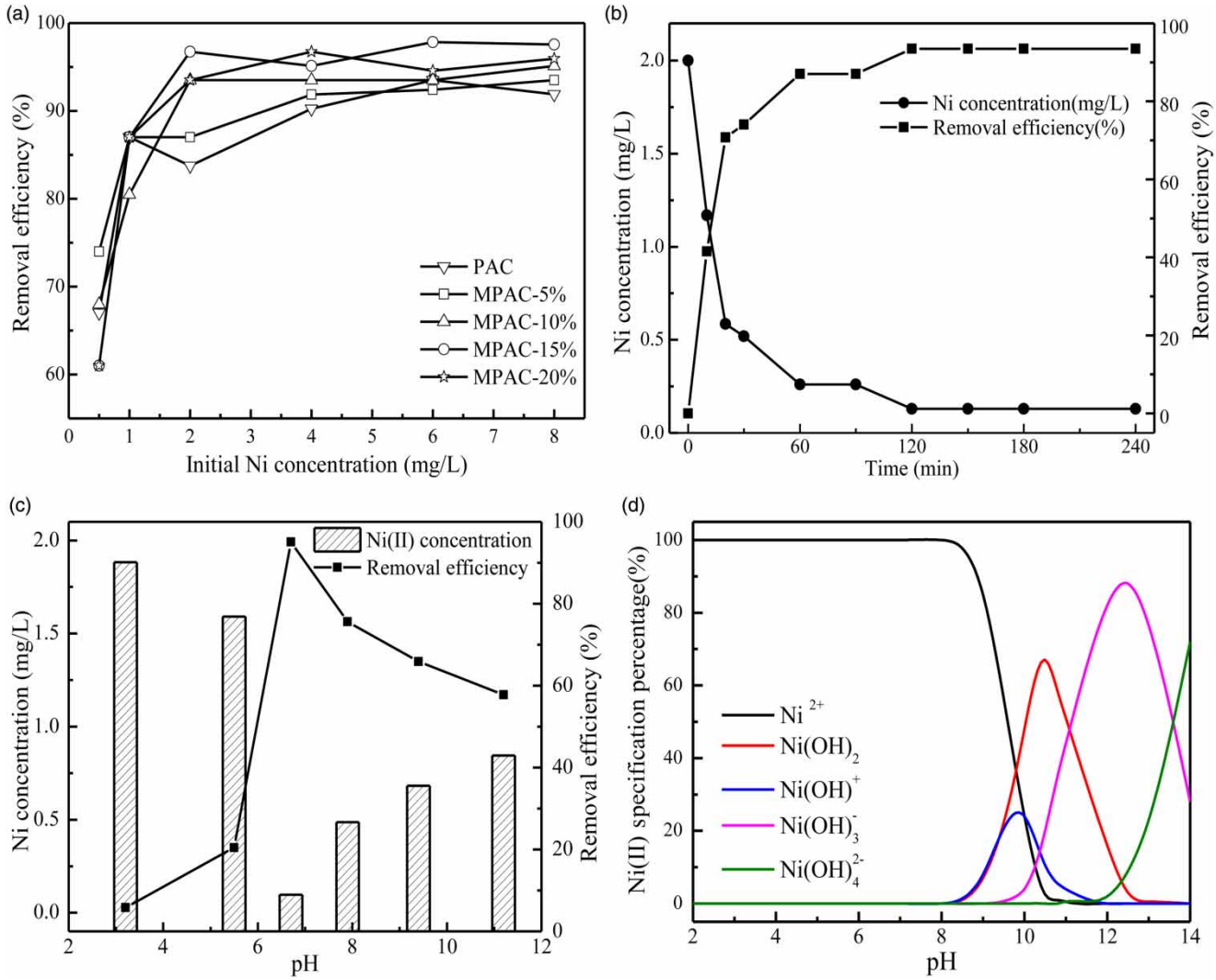

Figure 3 | Effect of (a) adsorbent types, (b) contact time and (c) pH on Ni(II) removal efficiency. (d) Nickel speciation at different pH.

higher than those in acidic condition. With the pH increase, the surface of MPA-15% was deprotonated and negatively charged. The high electrostatic force of attraction contributed to the adsorption of Ni(II); thus the adsorption efficiencies at pH equal to 7.9, 9.4 and 11.2 were all above 50%. As the concentration of OH^- increased, the solubility and species of Ni(II) were influenced and Ni^{2+} was partly replaced by $Ni(OH)^+$, $Ni(OH)_2$, $Ni(OH)_3^-$ and $Ni(OH)_4^{2-}$. The increased number of OH^- could combine with Ni(II) and retard the diffusion of Ni(II). Moreover, the competition of different species of Ni(II) also leads to the decrease of adsorption capacities and removal efficiencies in base conditions. Therefore, the removal of Ni(II) was much more favored by the neutral condition.

Adsorption kinetic and isotherm analysis

Adsorption kinetic analysis

The kinetics of Ni(II) adsorption onto MPAC-15% was verified using two different kinetic models based on the experimental data. The results are displayed in Figure 4 and Table 3.

Theoretically, the pseudo-first order model assumes that the adsorption rate of Ni is directly proportional to the difference between amount of Ni(II) adsorbed with time and the amount of Ni(II) adsorbed at equilibrium (Wu *et al.* 2018). From Table 3, the fitting R^2 for the pseudo-first order model was 0.9534 and the calculated adsorption amount at equilibrium was 1.95 mg/g. Thus,

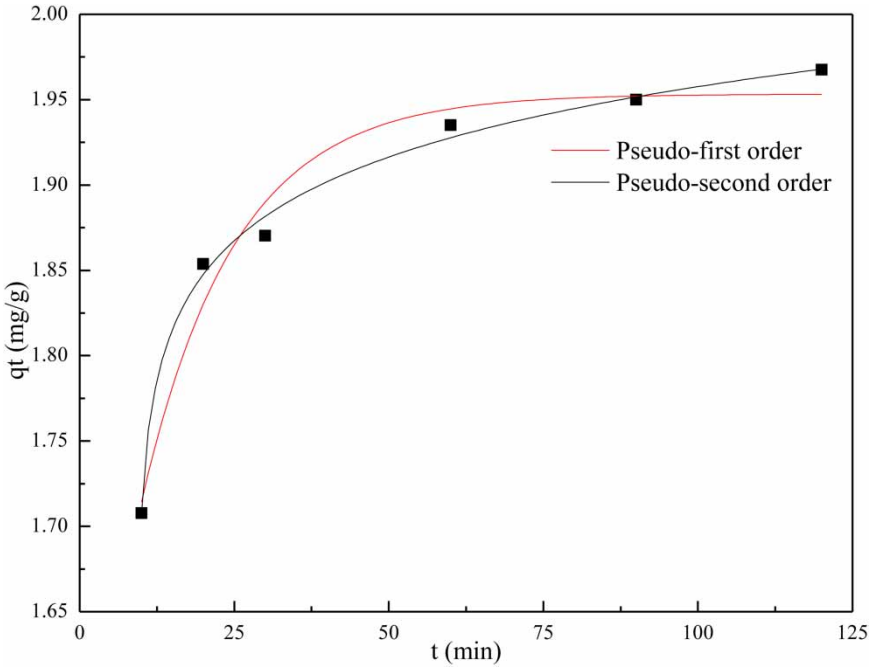

Figure 4 | Plots of pseudo-first order kinetic model and pseudo-second order kinetic model for the adsorption of Ni(II) by MPAC-15%.

Table 3 | Adsorption kinetic parameters of MPAC-15%

Kinetic model	Parameter	Value
Pseudo-first order model	q_e (mg/g)	1.95
	k_1 (min^{-1})	6.633×10^{-2}
	R^2	0.9534
Pseudo-second order model	q_e (mg/g)	1.72
	k_2	2.06×10^{-1}
	R^2	0.9920

the pseudo-first order could not illustrate the real reaction process. The pseudo-second order model is based on the assumption that the adsorption rate of Ni(II) is proportional to the square of the difference between the amount of Ni(II) adsorbed with time and amount of Ni(II) adsorbed at equilibrium. Compared with pseudo-first order model, pseudo-second order model had a much higher R^2, which was 0.9920. Thus, pseudo-second order model was more appropriate for this adsorption.

Adsorption isotherm analysis

To evaluate the characteristics of the adsorption process between liquid and solid phases when it reaches the equilibrium state, the adsorption isotherm study has been carried out. The results fitted by Langmuir and Freundlich are presented in Figure 5 and their corresponding constant factors resulting from the fitting figures are presented in Table 4.

Langmuir is a typical isotherm model that assumes all adsorption sites are 'equally active', the surface is energetically homogeneous and a monolayer surface coverage is formed without any interaction between the adsorbed molecules. Thus, there is a free-energy change for all adsorption sites considering no adsorbent–adsorbate interaction. The Freundlich isotherm model is based on the assumption that the adsorbent has a heterogeneous surface in nature and there is an increase in the concentration of the ionic species adsorbed on the surface of the solid when the concentration of certain species in the liquid phase is increased. In this model, the adsorption energy is assumed to exponentially decrease on the finishing point of the adsorption centers of adsorbents. The Temkin isotherm model takes into account the interaction of adsorbent–adsorbate. It assumes that heat of adsorption of all molecules in the layer would decrease linearly rather than logarithmically with coverage.

From the results of adsorption isotherms, the highest R^2 value was obtained for the Langmuir isotherm ($R^2 = 0.9874$). This result indicates that Ni(II) formed monolayer coverage on the prepared AC with the maximum monolayer adsorption capacity of 23.11 mg/g. This phenomenon means the surface of the adsorbent is homogenous in nature and every adsorption site has the same adsorption energy, with

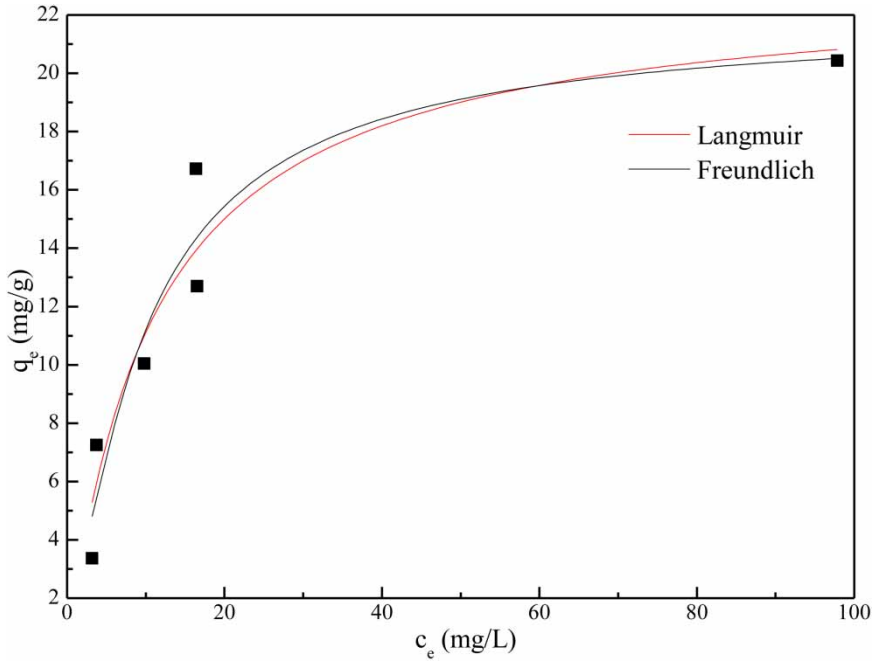

Figure 5 | Plots of Langmuir and Freundlich isotherm models for the adsorption of Ni(II) by MPAC-15%.

Table 4 | Adsorption isotherm parameters of MPAC-15%

	Langmuir		Freundlich	
R^2	0.9874		0.8698	
Constant	Q_{max}	23.11 mg/g	n	2.17
	K_L	0.093 L/mg	K_F	3.23 L/g

the energy constant related to the heat of adsorption value as 0.093 L/mg. According to equilibrium theory, an important factor that needs to be taken into account is R_L for the Langmuir isotherm. The equation for R_L can be described as Equation (7).

$$R_L = \frac{1}{1 + K_L C_0} \tag{7}$$

where K_L is the Langmuir isotherm constant and C_0 is the initial concentration of Ni(II) (mg/L). The value of R_L indicates the nature of the adsorption process corresponding to four cases: $R_L = 0$ for irreversible case, $0 < R_L < 1$ for favorable equilibrium, $R_L = 1$ for the linear case, and $R_L > 1$ for unfavorable equilibrium. R_L values from the given initial concentration range in this study have been calculated and found to be in a range of 0.05–0.35. These R_L values further confirm that MPAC-15% is favorable for the Ni(II) adsorption under the condition employed.

CONCLUSIONS

In this study, nitric acid MPAC was prepared and utilized for adsorption of Ni(II) in aqueous solution. The characterization analysis indicated PAC and MPACs were dominated by micropores and MPAC-15% was selected as the study adsorbent due to its relative high pore volume and surface area. SEM images showed that a large number of new pores presented on MPAC-15% surface and the pore width was mainly from 0.5 to 3.5 nm. The batch adsorption experiments revealed that MPACs achieved higher adsorption efficiency of Ni(II) than PAC with the help of newly generated surface acidic functional groups and MPAC-15% performs best. For the effect of contacting time, the adsorption sites of MPAC-15% for Ni(II) reached saturation at 120 min. Associating the surface functional groups in MPAC-15% and natural characters of Ni(II) with solution pH condition, neutral pH condition worked best for adsorption performance. Therefore, in order to reach the high adsorption efficiency, acid and alkaline conditions need to be avoided in MPAC-15% application. The kinetic fitting indicated that pseudo-second order adsorption model can fit the experiment data very well. Thus, Ni(II) adsorption by MPAC-15% was not only dominated by physical adsorption via highly developed micropores, but also affected by ion exchange between Ni(II) and functional groups on

MPAC-15% surface. Adsorption isotherm analysis illustrated the Langmuir model was favorable for the adsorption of Ni(II) process with $R^2 = 0.9874$ and maximum monolayer adsorption capacity of 23.11 mg/g.

ACKNOWLEDGEMENTS

This work was supported by Beijing Natural Science Foundation Fund (No. 8152025).

REFERENCES

Babel, S. & Kurniawan, T. A. 2004 Cr(VI) removal from synthetic wastewater using coconut shell charcoal and commercial activated carbon modified with oxidizing agents and/or chitosan. *Chemosphere* **54**, 951–967.

Bhatnagar, A., Hogland, W., Marques, M. & Sillanpää, M. 2013 An overview of the modification methods of activated carbon for its water treatment applications. *Chemical Engineering Journal* **219**, 499–511.

Ding, Z., Hu, X., Wan, Y., Wang, S. & Gao, B. 2016 Removal of lead, copper, cadmium, zinc, and nickel from aqueous solutions by alkali-modified biochar: batch and column tests. *Journal of Industrial and Engineering Chemistry* **33**, 239–245.

Ghaedi, M., Nasab, A. G., Khodadoust, S., Rajabi, M. & Azizian, S. 2014 Application of activated carbon as adsorbents for efficient removal of methylene blue: kinetics and equilibrium study. *Journal of Industrial and Engineering Chemistry* **20** (4), 2317–2324.

Gokce, Y. & Aktas, Z. 2014 Nitric acid modification of activated carbon produced from waste tea and adsorption of methylene blue and phenol. *Applied Surface Science* **313**, 352–359.

Gupta, V. K., Nayak, A., Agarwal, S., Chaudhary, M. & Tyagi, I. 2014 Removal of Ni(II) ions from water using scrap tire. *Journal of Molecular Liquids* **190**, 215–222.

Hu, Q., Liu, Y., Feng, C., Zhang, Z., Lei, Z. & Shimizu, K. 2018 Predicting equilibrium time by adsorption kinetic equations and modifying Langmuir isotherm by fractal-like approach. *Journal of Molecular Liquids* **268**, 728–733.

Hummel, W. & Curti, E. 2003 Nickel aqueous speciation and solubility at ambient conditions: a thermodynamic elegy. *Monatshefte für Chemie/Chemical Monthly* **134**, 941–973.

Ihsanullah, Abbas, A., Al-Amer, A. M., Laoui, T., Al-Marri, M. J., Nasser, M. S., Khraisheh, M. & Atieh, M. A. 2016 Heavy metal removal from aqueous solution by advanced carbon nanotubes: critical review of adsorption applications. *Separation and Purification Technology* **157**, 141–161.

Kong, J., Gu, R., Yuan, J., Liu, W., Wu, J., Fei, Z. & Yue, Q. 2018 Adsorption behavior of Ni(II) onto activated carbons from hide waste and high-pressure steaming hide waste. *Ecotoxicology and Environmental Safety* **156**, 294–300.

Kwon, J. S., Yun, S. T., Lee, J. H., Kim, S. O. & Jo, H. Y. 2010 Removal of divalent heavy metals (Cd, Cu, Pb, and Zn) and arsenic(III) from aqueous solutions using scoria: kinetics and equilibria of sorption. *Journal of Hazardous Materials* **174**, 307–313.

Li, C., Zhang, T. C., Liang, J. & Liang, Y. 2019 Removal of methyl orange wastewater by heterogeneous Fenton-like reaction over activated carbon pre-treated by nitric acid. *Desalination and Water Treatment* **145**, 393–398. https://doi.org/10.5004/dwt.2019.23738.

Liu, H., Zhang, J., Jiang, L., Kang, Y., Cheng, C., Guo, Z. & Zhang, C. 2015 Development of carbon adsorbents with high surface acidic and basic group contents from phosphoric acid activation of xylitol. *RSC Advances* **5**, 81220–81228.

MEPBB 2013 *Integrated Discharge Standard of Water Pollutants, Beijing DB11/307-2013*. Beijing Municipal Environmental Protection Bureau (MEPBB), China.

Monser, L. & Adhoum, N. 2009 Tartrazine modified activated carbon for the removal of Pb(II), Cd(II) and Cr(III). *Journal of Hazardous Materials* **161**, 263–269.

Moore, B. C., Cannon, F. S., Westrick, J. A., Metz, D. H., Shrive, C. A., DeMarco, J. & Hartman, D. J. 2001 Changes in GAC pore structure during full-scale water treatment at Cincinnati: a comparison between virgin and thermally reactivated GAC. *Carbon* **39** (6), 789–807.

NEPA 1989 *Water Quality–Determination of Nickel–Dimethylglyoxime Spectrophotometric Method*. China National Standard GB 11910. China National Environmental Protection Administration (NEPA).

NEPA 2008a *Test Method for Granular Activated Carbon from Coal–Determination of Iodine Number*. China National Standard GB/T 7702.7. China National Environmental Protection Administration (NEPA).

NEPA 2008b *Test Method for Granular Activated Carbon from Coal–Determination of Methylene Blue Adsorption*. China National Standard GB/T 7702.6. China National Environmental Protection Administration (NEPA).

Nightingale, E. R. 1959 Phenomenological theory of ion solvation. Effective radii of hydrated ions. *Journal of Physical Chemistry* **63**, 1381–1387.

Oladipo, A. A. & Gazi, M. 2015 Nickel removal from aqueous solutions by alginate-based composite beads: central composite design and artificial neural network modeling. *Journal of Water Process Engineering* **8**, e81–e91.

Peng, C., Jin, R., Li, G., Li, F. & Gu, Q. 2014 Recovery of nickel and water from wastewater with electrochemical combination process. *Separation and Purification Technology* **136**, 42–49.

Porto, M. B., Alvim, L. B. & de Almeida Neto, A. F. 2017 Nickel removal from wastewater by induced co-deposition using tungsten to formation of metallic alloys. *Journal of Cleaner Production* **142**, 3293–3299.

Rivera-Utrilla, J., Sánchez-Polo, M., Gómez-Serrano, V., Álvarez, P. M., Alvim-Ferraz, M. C. M. & Dias, J. M. 2011 Activated carbon modifications to enhance its water treatment applications: an overview. *Journal of Hazardous Materials* **187**, 1–23.

Shafeeyan, M. S., Daud, W. M. A. W., Houshmand, A. & Shamiri, A. 2010 A review on surface modification of activated carbon

for carbon dioxide adsorption. *Journal of Analytical and Applied Pyrolysis* **89**, 143–151.

Shim, J. W., Park, S. J. & Ryu, S.-K. 2001 Effect of modification with HNO_3 and NaOH on metal adsorption by pitch-based activated carbon fibers. *Carbon* **39**, 1635–1642.

Sing, K. S. 1985 Reporting physisorption data for gas/solid systems with special reference to the determination of surface area and porosity (Recommendations 1984). *Pure and Applied Chemistry* **57** (4), 603–619.

Su, P., Zhang, J. & Li, Y. 2019 Investigation of chemical associations and leaching behavior of heavy metals in sodium sulfide hydrate stabilized stainless steel pickling sludge. *Process Safety and Environmental Protection* **123**, 79–86.

Sun, N., Sun, C., Liu, J., Liu, H., Snape, C. E., Li, K., Wei, W. & Sun, Y. 2015 Surface modified spherical activated carbon materials for pre-combustion carbon dioxide capture. *RSC Advances* **5**, 33681–33690.

Uddin, M. K. 2017 A review on the adsorption of heavy metals by clay minerals, with special focus on the past decade. *Chemical Engineering Journal* **308**, 438–462.

Vunain, E., Mishra, A. K. & Mamba, B. B. 2016 Dendrimers, mesoporous silicas and chitosan-based nanosorbents for the removal of heavy-metal ions: a review. *International Journal of Biological Macromolecules* **86**, 570–586.

Wan, Z. & Li, K. 2018 Effect of pre-pyrolysis mode on simultaneous introduction of nitrogen/oxygen-containing functional groups into the structure of bagasse-based mesoporous carbon and its influence on Cu(II) adsorption. *Chemosphere* **194** 370–380.

Wu, H., Li, Z. & Liu, H. 2018 Development of carbon adsorbents with high surface acidity and basicity from polyhydric alcohols with phosphoric acid activation for Ni(II) removal. *Chemosphere* **206**, 115–121.

Xiao, Y., Xue, Y., Gao, F. & Mosa, A. 2017 Sorption of heavy metal ions onto crayfish shell biochar: effect of pyrolysis temperature, pH and ionic strength. *Journal of the Taiwan Institute of Chemical Engineers* **80**, 114–121.

Yang, R., He, S., Yi, J. & Hu, Q. 2016 Nano-scale pore structure and fractal dimension of organic-rich Wufeng-Longmaxi shale from Jiaoshiba area, Sichuan Basin: investigations using FE-SEM, gas adsorption and helium pycnometry. *Marine and Petroleum Geology* **70**, 27–45.

Yao, S., Zhang, J., Shen, D., Xiao, R., Gu, S., Zhao, M. & Liang, J. 2016 Removal of Pb(II) from water by the activated carbon modified by nitric acid under microwave heating. *Journal of Colloid and Interface Science* **463**, 118–127.

Yin, C. Y., Aroua, M. K. & Daud, W. M. A. W. 2007 Review of modifications of activated carbon for enhancing contaminant uptakes from aqueous solutions. *Separation and Purification Technology* **52**, 403–415.

Zhang, C., Peng, Y., Ning, K., Niu, X., Tan, S. & Su, P. 2014 Remediation of perfluoroalkyl substances in landfill leachates by electrocoagulation. *CLEAN–Soil, Air, Water* **42** (12), 1740–1743.

Zhang, C., Tan, S., Niu, X. & Su, P. 2015 Treatment of geothermal water with high fluoride content by electrocoagulation. *Desalination and Water Treatment* **54** (8), 2223–2227.

First received 30 April 2019; accepted in revised form 11 July 2019. Available online 22 July 2019